

In Search of Optimal Data Placement for Eliminating Write Amplification in Log-Structured Storage

Qiuping Wang[†], Jinhong Li[†], Patrick P. C. Lee[†], Guangliang Zhao^{*}, Chao Shi^{*}, Lilong Huang^{*}
[†]The Chinese University of Hong Kong ^{*}Alibaba Group

ABSTRACT

Log-structured storage has been widely deployed in various domains of storage systems for high performance. However, its garbage collection (GC) incurs severe write amplification (WA) due to the frequent rewrites of live data. This motivates many research studies, particularly on data placement strategies, that mitigate WA in log-structured storage. We show how to design an optimal data placement scheme that leads to the minimum WA with the future knowledge of block invalidation time (BIT) of each written block. Guided by this observation, we propose SepBIT, a novel data placement algorithm that aims to minimize WA in log-structured storage. Its core idea is to infer the BITs of written blocks from the underlying storage workloads, so as to place the blocks with similar estimated BITs into the same group in a fine-grained manner. We show via both mathematical and trace analyses that SepBIT can infer the BITs by leveraging the write skewness property in real-world storage workloads. Evaluation on block-level I/O traces from real-world cloud block storage workloads shows that SepBIT achieves the lowest WA compared to eight state-of-the-art data placement schemes.

1 INTRODUCTION

Modern storage systems adopt the *log-structured* design [24] for high performance. Examples include flash-based solid-state drives (SSDs) [1, 5], file systems [11, 17, 22, 24, 26], table stores [4], storage management [2], in-memory storage [25], RAID storage [14], and cloud block services [33]. Log-structured storage transforms random write requests into sequential disk writes in an append-only log, so as to reduce disk seek overhead and improve write performance. It also brings various advantages in addition to high write performance, such as improved flash endurance in SSDs [17], unified abstraction for building distributed applications [2, 4], efficient memory management in in-memory storage [25], and load balancing in cloud block storage [33].

The log-structured design writes live data blocks to the append-only log without modifying existing data blocks in-place, so it regularly performs *garbage collection* (GC) to reclaim the free space of stale blocks, by reading a segment of blocks, removing any stale blocks, and writing back the remaining live blocks. The repeated writes of live blocks lead to *write amplification* (WA), which incurs I/O interference to foreground workloads [14] and aggravates the I/O pressure to the underlying storage system.

Mitigating WA in log-structured storage has been a well-studied research topic in the literature (see §5 for details). In particular, a large body of studies focuses on designing *data placement* strategies by properly placing blocks in separate groups. He *et al.* [12] point out that a data placement scheme should group blocks by the *block invalidation time* (BIT) (i.e., the time when a block is

invalidated by a live block; a.k.a. the death time [12]) to achieve the minimum possible WA. However, without obtaining the future knowledge of the BIT pattern, how to design an optimal data placement scheme with the minimum WA remains an unexplored issue. Existing temperature-based data placement schemes that group blocks by block temperatures (e.g., write/update frequencies) [7, 16, 22, 27, 29, 35, 36] are arguably inaccurate to capture the BIT pattern and fail to group the blocks with similar BITs [12].

To this end, we propose SepBIT, a novel data placement scheme that aims to minimize the WA in log-structured storage. It infers the BITs of written blocks from the underlying storage workloads and separates the placement of written blocks into different groups, each of which stores the blocks with similar *estimated* BITs. Specifically, it builds on the *skewed* write patterns observed in real-world cloud block storage workloads at Alibaba Cloud [19]. It performs separation on the written blocks into *user-written blocks* and *GC-rewritten blocks* (defined in §2.1). It further performs separation on each set of user-written blocks and GC-rewritten blocks by inferring the BIT of each block, so as to perform more fine-grained separation of blocks into groups with similar estimated BITs. To the best of our knowledge, in contrast to existing temperature-based data placement schemes that group blocks by block temperatures [7, 16, 22, 27, 29, 35, 36], SepBIT is the first practical data placement scheme that groups blocks with similar BITs, backed by the analysis of real-world cloud block storage workloads. To summarize, this paper makes the following contributions:

- We first design an ideal data placement strategy that achieves the minimum WA in log-structured storage, based on the (impractical) assumption of having the future knowledge of BITs of written blocks. Our analysis not only motivates how to design a practical data placement scheme that aims to group the written blocks with similar BITs, but also provides an optimal baseline for our evaluation comparisons.
- We design SepBIT, which performs fine-grained separation of written blocks by inferring their BITs from the underlying storage workloads. We show via both mathematical and trace analyses that our BIT inference is effective in skewed workloads. We also show that SepBIT achieves low memory overhead in its indexing structure for tracking block statistics.
- We extensively evaluate SepBIT using the real-world cloud block storage workloads at Alibaba Cloud [19]. The workloads contain the block-level I/O traces of multiple volumes. We show that SepBIT achieves the lowest WA compared to eight state-of-the-art data placement schemes; for example, it reduces the overall WA by 8.6-15.9% and 9.1-20.2% when the Greedy [24] and Cost-Benefit [24, 25] algorithms are used for segment selection in GC, respectively. SepBIT also reduces the per-volume WA by up to 44.1%, compared to merely separating user-written and

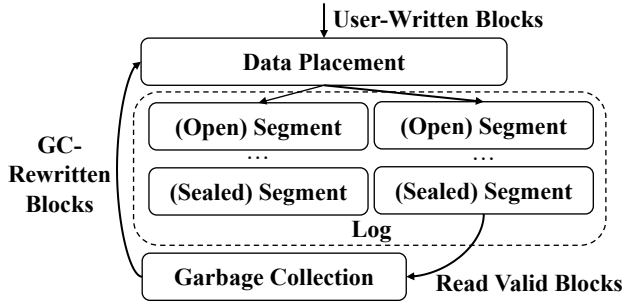


Figure 1: The workflow of a general data placement scheme.

GC-rewritten blocks in data placement.

2 BACKGROUND AND MOTIVATION

We introduce how GC works in log-structured storage and how we use data placement to mitigate WA in GC (§2.1). We then present an ideal data placement scheme that achieves the minimum WA, and state its limitations in practice (§2.2). Finally, we discuss the limitations in existing data placement schemes via trace analysis to motivate our design (§2.3).

2.1 GC in Log-Structured Storage

We consider a log-structured storage system that comprises multiple *volumes*, each of which is assigned to a user. Each volume is configured with a capacity of tens to hundreds of GiB and manages data in an append-only manner. It is further divided into *segments* that are configured with a maximum size (e.g., tens to hundreds of MiB). Each segment contains fixed-size *blocks*, each of which is identified by a *logical block address (LBA)* and has a size (e.g., several KiB) that aligns with the underlying disk drives. Each block, either from a new write or from an update to an existing block, is appended to a segment (called an *open* segment) that has not yet reached its maximum size. If a segment reaches its maximum size, the segment (called a *sealed* segment) becomes immutable. Updating an existing block is done in an *out-of-place* manner, in which the latest version of the block is appended to an open segment and becomes a *valid* block, while the old version of the block is invalidated and becomes an *invalid* block.

Log-structured storage needs to regularly reclaim the space occupied by the invalid blocks via GC. A variety of GC policies can be realized, yet we can abstract a GC policy as a three-phase procedure:

- *Triggering*, which decides when a GC operation should be activated. In this work, we assume that a GC operation is triggered for a volume when its *garbage proportion (GP)* (i.e., the fraction of invalid blocks among all valid and invalid blocks) exceeds a pre-defined threshold (e.g., 15%).
- *Selection*, which selects one or multiple sealed segments for GC. In this work, we focus on two selection algorithms: (i) Greedy [24], which selects the sealed segments with the highest GPs, and (ii) Cost-Benefit [24, 25], which selects the sealed segments that have the highest values $\frac{GP \cdot age}{1 - GP}$ (where *age* refers to the elapsed time of a sealed segment since it is sealed) for GC.
- *Rewriting*, which discards all invalid blocks from the selected

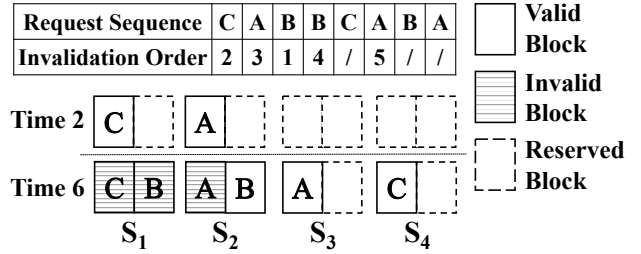


Figure 2: Example of the ideal data placement scheme.

sealed segments and writes back the remaining valid blocks into one or multiple open segments. The space of the selected sealed segments can be reused.

A log-structured storage system sees two types of written blocks: in addition to the *user-written* blocks issued from either a new write or an update, there are also *GC-rewritten blocks* due to the rewrites of the valid blocks during GC. Thus, GC inevitably incurs *write amplification (WA)*, defined as the ratio of the total number of both user-written blocks and GC-rewritten blocks to the number of user-written blocks. To avoid aggravating the I/O pressure to the storage system, it is critical to minimize WA.

In this work, we aim to design a proper data placement scheme that mitigates the WA due to GC. Figure 1 shows the workflow of a general data placement scheme, which separates all written blocks (i.e., user-written and GC-rewritten blocks) into different groups and writes the blocks to the open segments of the respective groups. The data placement scheme is compatible with any GC policy (i.e., independent of the triggering, selection, and rewriting policies).

2.2 Ideal Data Placement

We present an ideal data placement scheme that minimizes WA (i.e., $WA=1$). We also elaborate why it is infeasible to realize in practice, so as to motivate the design of an effective practical data placement scheme.

System model. We first define the notations. Consider a write-only request sequence of blocks that are written to a log-structured storage system. Let m be the number of blocks in the request sequence and s be the segment size (in units of blocks). Let $k = \lceil \frac{m}{s} \rceil$ be the number of sealed segments in the system, and let S_1, S_2, \dots, S_k denote the corresponding k sealed segments. Let o_i (where $o_i \geq 1$) be the *invalidation order* of the i -th block in the request sequence based on the BITs of all blocks (where $1 \leq i \leq m$), meaning that the i -th block is the o_i -th invalidated block among all invalid blocks.

Placement design. For the ideal placement scheme, we make the following assumptions. Suppose that the system has the future knowledge of the BITs of all blocks, and hence the invalidation order o_i of the i -th block in the request sequence (where $1 \leq i \leq m$). It also allocates k open segments for storing incoming blocks, and performs a GC operation whenever there are s invalid blocks in the system (i.e., one segment size of invalid blocks).

The system writes the i -th block to the $\lceil \frac{o_i}{s} \rceil$ -th open segment. If the j -th (where $1 \leq j \leq k$) open segment is full, it is sealed into the sealed segment S_j . Thus, S_j stores the blocks with the invalidation orders in the range of $[(j-1) \cdot s + 1, j \cdot s]$. The first GC operation is triggered when there exist s invalid blocks; according to the

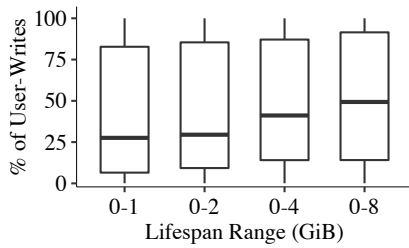


Figure 3: Percentages of user-written blocks with different short lifespans.

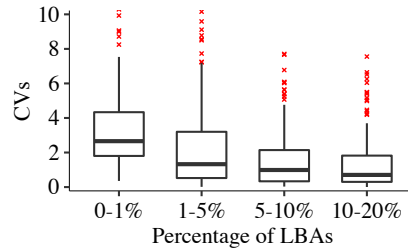


Figure 4: CVs of the lifespans of frequently updated blocks with different similar update frequencies.

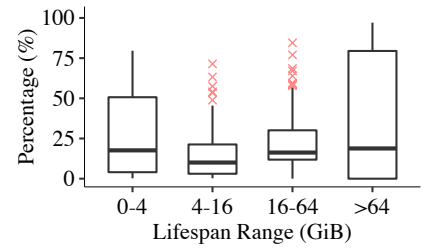


Figure 5: Percentages of rarely updated blocks with different lifespans.

placement, all such blocks must be stored in S_1 . Thus, the first GC operation will choose S_1 for GC, and there will be no rewrites as all blocks in S_1 must be invalid. In general, the j -th GC operation (where $1 \leq j \leq k$) will choose S_j for GC, and there will be no rewrites as S_j contains only invalid blocks.

Figure 2 depicts an example of the ideal data placement scheme. Consider a write-only request sequence with $m = 8$ blocks with three LBAs A , B , and C . We fix the segment size as $s = 2$. We show the status of the volume at time 2 and time 6 when the second block and sixth block are written, respectively. At time 2, we have appended C to S_1 and A to S_2 , as their invalidation orders are 2 and 3, respectively. Note that all blocks in S_1 become invalid when the third block is written at time 3, and at this time we can perform a GC operation to reclaim the free space occupied by S_1 . Note that the GC operation does not incur any rewrite. Later, at time 6, the system appends A to S_3 since its invalidation order is 5.

Limitations and lessons learned. While the ideal data placement scheme achieves the minimum WA, there exist two practical limitations. First, the scheme needs to have future knowledge of the BIT of every block to assign the blocks to the corresponding open segments, but having such future knowledge is infeasible in practice. Second, the scheme needs to provision $k = \lceil m/s \rceil$ open segments to hold all m blocks in the request sequence in the worst case, thereby incurring high memory overhead as m increases. Having too many open segments also incurs substantial random writes that lead to performance slowdown.

A practical data placement scheme should address the above two limitations. Without the future knowledge of BITs, it should effectively *infer* the BIT of each written block. With only a limited number of available open segments, it should group written blocks by *similar BITs* instead of placing them in strict invalidation order. Our goal is to address the limitations driven by real-world cloud block storage workloads.

2.3 Motivation

We show via trace analysis that existing data placement schemes cannot accurately capture the BIT pattern and group the blocks with similar BITs for the effective WA mitigation [12]. Specifically, we consider 186 volumes from a real-world cloud block storage system (§4.2) and analyze the lifetime of each user-written block. We define the *lifespan* of a block as the number of user-written bytes in the whole workload since it is first written until it is invalidated (or until the end of the traces). We make three key observations.

Observation 1: User-written blocks generally have short lifespans. We say that a block has a short lifespan if its lifespan is smaller than the write working set size (WSS) (i.e., the number of unique written LBAs multiplied by the 4 KiB block size). In our traces, each volume typically has a write WSS of at least 10 GiB. We examine the percentages of user-written blocks that fall into different lifespan range groups with short lifespans that are smaller than 10 GiB. Figure 3 shows the boxplots of the percentages over all volumes. We find that in a large fraction of volumes, their user-written blocks tend to have short lifespans. For example, half of the volumes have more than 49.3% of user-written blocks with lifespans shorter than 8 GiB, and have more than 27.6% of user-written blocks with lifespans shorter than 1 GiB. In contrast, GC-rewritten blocks generally have long lifespans as they are not updated before GC.

Our findings show that user-written blocks and GC-rewritten blocks can have vastly different BIT patterns, in which user-written blocks tend to have short lifespans, while GC-rewritten blocks tend to have long lifespans. Existing data placement schemes either mix user writes and GC writes [7, 16, 22, 29], or focus on user writes [27, 35, 36], in the data placement decisions. Failing to distinguish between user-written blocks and GC-rewritten blocks can lead to inefficient WA mitigation. Instead, it is critical to separately identify the BIT patterns of user-written blocks and GC-rewritten blocks.

Observation 2: Frequently updated blocks have highly varying lifespans. We investigate *frequently updated blocks*, referred to as the blocks whose *update frequencies* (i.e., the number of updates) rank top 20% in the write working set (i.e., the set of LBAs being written) of a volume. Specifically, for each volume, we divide the frequently updated blocks into four groups, namely top 1%, top 1-5%, top 5-10%, and top 10-20%, so that the blocks in each group have similar update frequencies. To avoid evaluation bias, we exclude the blocks that have not been invalidated before the end of the traces. For each group of a volume, we calculate the *coefficient of variance (CV)* (i.e., the standard deviation divided by the mean) of the lifespans of the blocks; a high CV (e.g., larger than one) implies that the lifespans have high variance.

Figure 4 shows the boxplots of the CVs in each group across all volumes. We observe that frequently updated blocks with similar update frequencies have high variance in their lifespans (and hence the BITs); for example, 25% of the volumes have their CVs exceeding 4.34, 3.20, 2.14, and 1.82 in the four groups top 1%, top 1-5%, top 5-10%, and top 10-20%, respectively. Our findings also suggest that existing temperature-based data placement schemes that group the blocks with similar write/update frequencies [7, 16, 22, 27, 29, 35, 36]

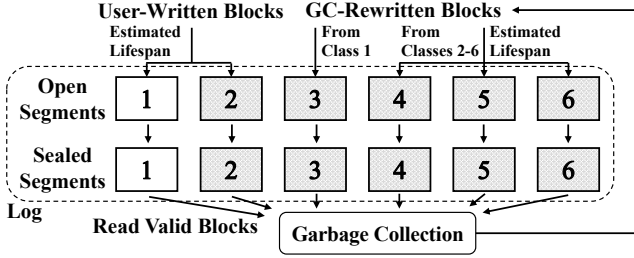


Figure 6: SepBIT workflow.

cannot effectively group blocks with similar BITs, and hence the WA cannot be fully mitigated.

Observation 3: Rarely updated blocks dominate and have highly varying lifespans. We examine the write working set of each of the 186 volumes and define the *rarely updated blocks* as those that are updated no more than four times during the one-month trace period. We observe that rarely updated blocks occupy a high percentage in the write working sets of a large fraction of volumes. Specifically, in half of the volumes, more than 72.4% of their write working sets contain rarely updated blocks. We further investigate the lifespans of those rarely updated blocks. For each volume, we divide the rarely updated blocks into four groups that are partitioned by the lifespans of 4 GiB, 16 GiB, and 64 GiB. We then calculate the percentage of those blocks that fall into each group.

Figure 5 shows the boxplots of the percentages of rarely updated blocks in different groups of lifespans across all volumes. We see that in 25% of the volumes, more than 50.7% of the rarely updated blocks have their lifespans shorter than 4 GiB. Also, for all groups of lifespans, the percentages are non-negligible (e.g., all groups have their medians larger than 10.0%). In other words, rarely updated blocks have large deviations of lifespans (and hence BITs) in a volume. As in Observation 2, our findings again suggest that existing temperature-based data placement schemes cannot effectively group the rarely updated blocks with similar BITs. Rarely updated blocks are often treated as cold blocks with low write frequencies, so they tend to be grouped together and separated from the hot blocks with high write frequencies. However, their vast differences in BIT patterns make temperature-based data placement schemes inefficient in mitigating WA.

3 SEPBIT DESIGN

We present SepBIT, a novel data placement scheme aiming for minimizing WA in log-structured storage systems. We first present an overview of SepBIT (§3.1). We then show how we infer the BITs of both user-written blocks (§3.2) and GC-rewritten blocks (§3.3) using both mathematical and trace analyses. We provide the implementation details of SepBIT, especially on how it separates blocks on-the-fly (§3.4).

3.1 Design Overview

SepBIT works by separating blocks into different *classes* of segments via inferring the BITs of user-written and GC-rewritten blocks, such that the blocks with similar estimated BITs are grouped together in the same class. Figure 6 depicts the workflow of SepBIT. Our current

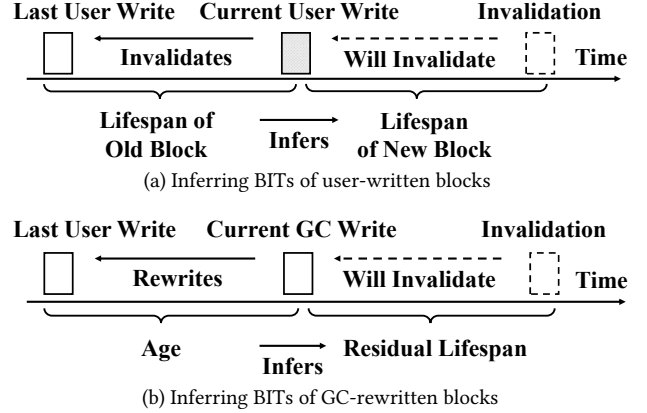


Figure 7: Ideas of inferring BITs in SepBIT.

design of SepBIT defines *six* classes of segments, in which Classes 1-2 correspond to the segments of user-written blocks, while Classes 3-6 correspond to the segments of GC-rewritten blocks. Each class is now configured with one open segment and has multiple sealed segments. If an open segment reaches the maximum size, it is sealed and remains in the same class.

SepBIT infers the lifespans (defined in §2.3) of blocks, and in turn infers the corresponding BITs of blocks. For user-written blocks (i.e., Classes 1-2), SepBIT stores the *short-lived* blocks (with short lifespans) in Class 1 and the remaining *long-lived* blocks (with long lifespans) in Class 2. For GC-rewritten blocks (i.e., Classes 3-6), SepBIT appends the blocks from Class 1 that are rewritten by GC into Class 3, and groups the remaining GC-rewritten blocks into Classes 4-6 by similar BITs being inferred.

The design intuition behind SepBIT is as follows. For each user-written block, SepBIT examines its *last user write time* to infer its lifespan. If the user-written block is issued from a new write, SepBIT assumes that it has an infinite lifespan. Otherwise, if the user-written block updates an old block, SepBIT uses the lifespan of the old block (i.e., the number of user-written bytes in the whole workload since its last user write time until it is now invalidated) to estimate the lifespan of the user-written block, as shown in Figure 7(a). Our intuition is that *any user-written block that invalidates a short-lived block is also likely to be a short-lived block* (§3.2). Then if the short-lived blocks are written at about the same time, their corresponding BITs will be close, so SepBIT groups them into same class (i.e., Class 1). For the long-lived blocks (including the user-written blocks from new writes), SepBIT groups them into Class 2.

For each GC-rewritten block, SepBIT examines its *age*, defined as the number of user-written bytes in the whole workload since its last user write time until it is rewritten by GC, to infer its *residual lifespan*, defined as the number of user-written bytes since it is rewritten by GC until it is invalidated (or until the end of the traces), as shown in Figure 7(b). As a result, the lifespan of a GC-rewritten block is its age plus its residual lifespan. Our intuition is that *any GC-rewritten block with a smaller age has a higher probability to have a short residual lifespan* (§3.3), implying that GC-rewritten blocks with different ages are expected to have different residual lifespans. Thus, SepBIT can distinguish the blocks of different residual lifespans

based on their ages and group the GC-rewritten blocks with similar ages into the same classes.

Our design intuition builds on the assumption that the access pattern is *skewed*, so as to infer the BITs of blocks for data placement. We justify our assumption and verify the effectiveness of SepBIT via the mathematical analysis for skewed distributions and the trace analysis from real-world cloud block storage workloads (§3.2 and §3.3). To adapt to changing workloads and GC policies, SepBIT dynamically monitors the workloads to separate user-written blocks and GC-rewritten blocks into different classes (§3.4).

3.2 Inferring BITs of User-Written Blocks

We show via both mathematical and trace analyses the effectiveness of SepBIT in estimating the BITs of user-written blocks based on the lifespans. Let n be the total number of unique LBAs in a working set; without loss of generality, each LBA is denoted by an integer from 1 to n . Let p_i (where $1 \leq i \leq n$) be the probability that LBA i is being written. Consider a write-only request sequence of blocks, each of which is associated with a sequence number b and the corresponding LBA A_b . Let b and b' (where $b' < b$) denote the sequence numbers of a new user-written block and the corresponding invalid old block, respectively (i.e., $A_b = A_{b'}$).

Recall from §3.1 that SepBIT estimates the lifespan (denoted by u) of the user-written block b using the lifespan (denoted by v) of the old block b' , so the estimated BIT of block b is equal to the current user write time plus the estimated lifespan u ; note that both u and v are expressed in units of blocks. We claim that if v is small, u is also likely to be small. To validate the claim, let u_0 and v_0 (both in units of blocks) be two thresholds. We then examine the conditional probability of $u \leq u_0$ given the condition that $v \leq v_0$ subject to a workload of a different skewness. If the conditional probability is high for small u_0 and v_0 , then our claim holds.

Mathematical analysis. Formally, we investigate the following conditional probability:

$$\Pr(u \leq u_0 \mid v \leq v_0) = \frac{\Pr(u \leq u_0 \text{ and } v \leq v_0)}{\Pr(v \leq v_0)},$$

where the denominator is expressed as:

$$\begin{aligned} \Pr(v \leq v_0) &= \sum_{i=1}^n \Pr(v \leq v_0 \mid A_{b'} = i) \cdot \Pr(A_{b'} = i) \\ &= \sum_{i=1}^n (1 - (1 - p_i)^{v_0}) \cdot p_i, \end{aligned}$$

and the numerator is expressed as:

$$\begin{aligned} \Pr(u \leq u_0 \text{ and } v \leq v_0) &= \sum_{i=1}^n \Pr(u \leq u_0 \text{ and } v \leq v_0 \mid A_b = i) \cdot \Pr(A_b = i) \\ &= \sum_{i=1}^n (1 - (1 - p_i)^{u_0}) \cdot (1 - (1 - p_i)^{v_0}) \cdot p_i. \end{aligned}$$

We analyze the conditional probability via the Zipf distribution, in which we set $p_i = (1/i^\alpha) / \sum_{j=1}^n (1/j^\alpha)$, where $1 \leq i \leq n$ for some non-negative skewness parameter α . A larger α implies a more skewed distribution. Here, we fix $n = 10 \times 2^{18}$, which corresponds to a working set of 10 GiB with 4 KiB blocks. We then study how the conditional probability $\Pr(u \leq u_0 \mid v \leq v_0)$ varies across u_0 , v_0 , and α .

Figure 8(a) first shows the conditional probability for varying u_0 and v_0 , where we fix $\alpha = 1$. We focus on short lifespans by varying

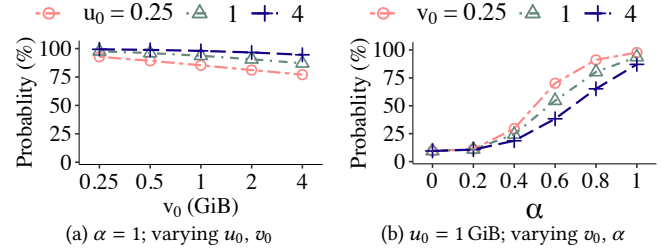


Figure 8: Inferring BITs of user-written blocks: $\Pr(u \leq u_0 \mid v \leq v_0)$ versus v_0 and α .

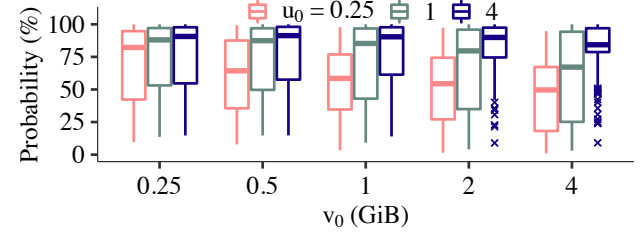


Figure 9: Inferring BITs of user-written blocks: Boxplots of $\Pr(u \leq u_0 \mid v \leq v_0)$ for different u_0 and v_0 in real-world workloads.

u_0 and v_0 of up to 4 GiB, which is less than the write WSS (§2.3). Overall, the conditional probability is high for different u_0 and v_0 ; the lowest one is 77.1% for $v_0 = 4$ GiB and $u_0 = 0.25$ GiB. This shows that a user-written block is highly likely to have a short lifespan if its invalidated block also has a short lifespan. In particular, the conditional probability is higher if v_0 is smaller (i.e., the invalidated blocks have shorter lifespans), implying a more accurate estimation of the lifespan of the user-written block.

Figure 8(b) next shows the conditional probability for varying v_0 and α , where we fix $u_0 = 1$ GiB. Note that for $\alpha = 0$, the Zipf distribution reduces to a uniform distribution. Overall, the conditional probability increases with α (i.e., for a more skewed distribution). For example, for $\alpha = 1$, the conditional probability is at least 87.1%. On the other hand, for $\alpha = 0$, the conditional probability is only 9.5%. This indicates that the high accuracy of lifespan estimation only holds under skewed workloads.

Trace analysis. We use the block-level I/O traces from Alibaba Cloud (§4.2) to validate if the conditional probability remains high in real-world workloads. To compute the conditional probability, we first find out the set of user-written blocks that invalidate old blocks with $v \leq v_0$. Then the conditional probability is the fraction of blocks with $u \leq u_0$ in the set. Figure 9 shows the boxplots of the conditional probabilities over all volumes for different u_0 and v_0 . In general, the conditional probability remains high in most of the volumes. For example, for $v_0 = 4$ GiB, the medians of the conditional probabilities are in the range of 49.6-84.3%, and the 75th percentiles are in the range of 67.3-96.7%. Also, the conditional probability tends to be higher for a smaller v_0 .

3.3 Inferring BITs of GC-Rewritten Blocks

We further show via both mathematical and trace analyses the effectiveness of SepBIT in estimating the BITs of GC-rewritten blocks based on the *residual* lifespans. Recall from §3.1 that SepBIT estimates the residual lifespan of a GC-rewritten block using its

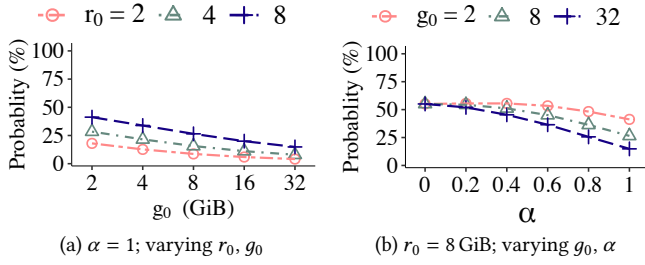


Figure 10: Inferring BITs of GC-rewritten blocks: $\Pr(u \leq g_0 + r_0 \mid u \geq g_0)$ versus g_0 and α .

age, so the estimated BIT of the GC-rewritten block is equal to the current GC write time plus the estimated residual lifespan. However, characterizing directly GC-rewritten blocks is non-trivial, as it depends on the actual GC policy (e.g., when GC is triggered and which segments are selected for GC) (§2.1). Instead, we model GC-rewritten blocks based on user-written blocks. If a user-written block has a lifespan above a certain threshold, we assume that it is rewritten by GC and treat it as a GC-rewritten block with an age equal to the threshold. We can then apply a similar analysis for user-written blocks as in §3.2.

We define the following notations. As each GC-rewritten block is a user-written block before being rewritten by GC, we identify each GC-rewritten block by its corresponding user-written block with sequence number b . Let u , g , and r be its lifespan, age, and residual lifespan, respectively, such that $u = g + r$; each of the variables is measured in units of blocks. We claim that r has a higher probability to be small with a smaller g . To validate the claim, let g_0 and r_0 (both in units of blocks) be the thresholds for the age and the residual lifespan, respectively. We examine the conditional probability of $u \leq g_0 + r_0$ given the condition that $u \geq g \geq g_0$ subject to a workload of different skewness. The conditional probability specifies the fraction of GC-rewritten blocks whose residual lifespans are shorter than r_0 among all GC-rewritten blocks with age g_0 (note that the GC-rewritten blocks are modeled as user-written blocks with lifespans above g_0). If the conditional probability is higher for a smaller g_0 subject to a fixed r_0 , then our claim holds.

Mathematical analysis. Formally, we investigate the following conditional probability:

$$\Pr(u \leq g_0 + r_0 \mid u \geq g_0) = \frac{\Pr(g_0 \leq u \leq g_0 + r_0)}{\Pr(u \geq g_0)},$$

where the numerator and denominator correspond to all user-written blocks whose lifespans range from $g_0 \leq u \leq g_0 + r_0$ and $u \geq g_0$, respectively. According to the computation in §3.2, the numerator and denominator are respectively:

$$\Pr(g_0 \leq u \leq g_0 + r_0) = \sum_{i=1}^n p_i \cdot ((1 - p_i)^{g_0} - (1 - p_i)^{g_0 + r_0})$$

$$\text{and } \Pr(u \geq g_0) = \sum_{i=1}^n p_i \cdot (1 - p_i)^{g_0}.$$

As in §3.2, we use the Zipf distribution and fix $n = 10 \times 2^{18}$ unique LBAs. We study how the conditional probability $\Pr(u \leq g_0 + r_0 \mid u \geq g_0)$ varies across g_0 , r_0 , and α .

Figure 10(a) first shows the conditional probability for varying g_0 and r_0 , where we fix $\alpha = 1$. We focus on a large value of g_0 of up to 32 GiB since we target long-lived blocks. We also vary r_0 up to

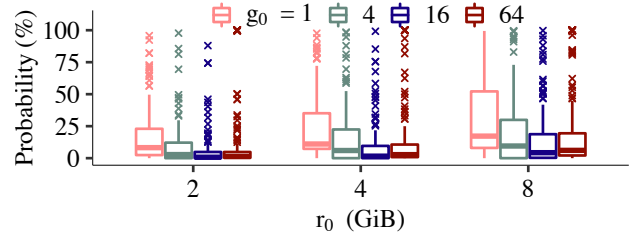


Figure 11: Inferring BITs of GC-rewritten blocks: Boxplots of $\Pr(u \leq g_0 + r_0 \mid u \geq g_0)$ for different r_0 and g_0 in real-world workloads.

8 GiB. Overall, for a fixed r_0 , the conditional probability decreases as g_0 increases. For example, given that $r_0 = 8$ GiB, the probability with $g_0 = 2$ GiB is 41.2%, while the probability for $g_0 = 32$ GiB drops to 14.9%. This validates our claim that GC-rewritten blocks with different ages are expected to have different residual lifespans. Thus, we can distinguish the GC-rewritten blocks of different residual lifespans based on their ages.

Figure 10(b) further shows the conditional probability for varying g_0 and α , where we fix $r_0 = 8$ GiB. For a small α , the conditional probability has a limited difference for varying g_0 , while the difference becomes more significant as α increases. For example, for $\alpha = 0$ (i.e., the uniform distribution), there is no difference varying g_0 ; for $\alpha = 0.2$, the difference of the conditional probability between $g_0 = 2$ GiB and $g_0 = 32$ GiB is only 3.5%, while the difference for $\alpha = 1$ is 26.4%. This indicates that our claim holds under skewed workloads, and we can better distinguish the GC-rewritten blocks of different residual lifespans under more skewed workloads.

Trace analysis. We also use block-level I/O traces from Alibaba Cloud (§4.2) to examine the conditional probability in real-world workloads. We first identify the set of blocks with $u \geq g_0$ in the workload, and then compute the conditional probability as a fraction of blocks with $u \leq g_0 + r_0$ in the set. Figure 11 depicts the boxplots of the conditional probabilities over all volumes for different g_0 and r_0 . For a fixed r_0 , the conditional probabilities have significant differences for varying g_0 . For example, if g_0 increases from 1 GiB to 16 GiB and we fix $r_0 = 8$ GiB, the 75th percentiles of probabilities drop from 52.2% to 18.7%.

3.4 Implementation Details

We describe how to tune the thresholds for separating blocks into different classes. We also provide the algorithmic details of SepBIT and discuss its memory usage.

Threshold selection. We assign blocks into different classes by their estimated BITs with multiple thresholds: for user-written blocks, we define a *lifespan threshold* for separating short-lived blocks and long-lived blocks; for GC-rewritten blocks, we need multiple *age thresholds* to separate them by ages (§3.1). We configure the thresholds via the *segment lifespan* of a segment, defined as the number of user-written bytes in the workload since the segment is created (i.e., the time when the first block is appended to the segment) until it is reclaimed by GC. Specifically, we monitor the average segment lifespan, denoted by ℓ , among a fixed number of recently reclaimed segments in Class 1. For each user-written block, if it invalidates an old block with a lifespan less than ℓ , we write

Algorithm 1 SepBIT

```
1:  $t = 0; \ell = +\infty; \ell_{tot} = 0; n_c = 0$ , where  $t$  is the global timestamp
2: function GarbageCollect()
3:   Select a segment  $S$  by selection algorithm
4:   if  $S$  is from Class 1 then
5:      $n_c = n_c + 1, \ell_{tot} = \ell_{tot} + (t - S.creation\_time)$ 
6:   end if
7:   if  $n_c = 16$  then
8:      $\ell = \ell_{tot}/n_c; n_c = 0; \ell_{tot} = 0$ 
9:   end if
10:  for each valid user-written block  $b$  in  $S$  do
11:    GCWrite( $b$ )
12:  end for
13: end function
14: function UserWrite( $b$ )
15:  Find lifespan  $v$  of the invalidated block  $b'$  due to  $b$ 
16:  if  $v < \ell$  then
17:    Append  $b$  to open segment of Class 1
18:  else
19:    Append  $b$  to open segment of Class 2
20:  end if
21:   $t = t + 1$ 
22: end function
23: function GCWrite( $b$ )
24:  if  $b$  is from Class 1 then
25:    Append  $b$  to open segment of Class 3
26:  else
27:     $g = t - b$ 
28:    If  $g \in [0, 4\ell)$ , append  $b$  to open segment of Class 4
29:    If  $g \in [4\ell, 16\ell)$ , append  $b$  to open segment of Class 5
30:    If  $g \in [16\ell, +\infty)$ , append  $b$  to open segment of Class 6
31:  end if
32: end function
```

it to Class 1; otherwise, we write it to Class 2. For GC-rewritten blocks, we set the age thresholds as multiples of ℓ (see below).

Algorithmic details. Algorithm 1 shows the pseudo-code of SepBIT, which consists of three functions: GarbageCollect, UserWrite, and GCWrite. Each class always corresponds to one open segment. If an open segment is full, it becomes a sealed segment, and SepBIT creates a new open segment within the same class. SepBIT initializes the average segment lifespan $\ell = +\infty$, which is updated on-the-fly. It also tracks a global timestamp t , which records the sequence number of the current user-written block.

GarbageCollect is triggered by a GC operation according to the GC policy (§2.1). It performs GC and monitors the runtime information of the reclaimed segments. It selects a segment S for GC based on the selection algorithm (e.g., Greedy or Cost-Benefit (§2.1)). It sums up the lifespans of collected segments from Class 1 as ℓ_{tot} , and computes the average lifespan $\ell = \ell_{tot}/n_c$ for every fixed number n_c (e.g., $n_c = 16$ in our current implementation) of reclaimed segments.

UserWrite processes each user-written block b . It first computes the lifespan v of the invalidated old block b' . If v is less than ℓ , UserWrite appends b (which is treated as a short-lived block) to the open segment of Class 1; otherwise, it appends b (which is treated as a long-lived block) to the open segment of Class 2.

GCWrite processes each GC-rewritten block that corresponds

to some user-written block b . If b is originally stored in Class 1, GCWrite appends b to the open segment of Class 3; otherwise, GCWrite appends b to one of the open segments of Classes 4-6 based on the age of b . Currently, we configure the age thresholds as three ranges, $[0, 4\ell)$, $[4\ell, 16\ell)$, and $[16\ell, +\infty)$, for Classes 4-6, respectively, based on our evaluation findings. Nevertheless, we have also experimented with different numbers of classes and thresholds, and we observe only marginal differences in WA.

Memory usage. SepBIT only stores the last user write time of each block as the metadata alongside the block *on disk*, without maintaining a mapping from every LBA to its last user write time in memory. Specifically, for user-written blocks, SepBIT only needs to know whether the lifespan of the invalidated block is shorter than a threshold. It is thus sufficient for SepBIT to track only the recently written LBAs in a first-in-first-out (FIFO) queue in memory. In our current implementation, SepBIT dynamically adjusts the queue length according to the value ℓ . If the FIFO queue is full, each insert of an element will dequeue one element from the queue. If ℓ increases, the FIFO queue allows more inserts without dequeuing any element; if ℓ decreases, the FIFO queue dequeues two elements for each insert until the number of elements drops below ℓ . If the LBA exists in the FIFO queue and its user write time is within the recent ℓ user writes, SepBIT writes it into Class 1.

On the other hand, for GC-rewritten blocks, SepBIT retrieves them during GC and can examine the user write time directly from the metadata of each GC-rewritten block, so as to assign the GC-rewritten block to the corresponding class without any memory overhead incurred.

4 EVALUATION

We evaluate SepBIT via trace-driven simulation using real-world cloud block storage traces, by comparing SepBIT with eight existing data placement schemes.

4.1 Data Placement Schemes

We compare SepBIT with eight existing temperature-based data placement schemes, namely Dynamic dAta Clustering (DAC) [7], SFS [22], MultiLog (ML) [22], extent-based identification (ETI) [27], MultiQueue (MQ) [35], Sequentiality, Frequency, and recency (SFR) [35], Fading Average Data Classifier (FADaC) [16], and WARCIP [36]. Take DAC [7] as an example. DAC associates each LBA with a temperature-based counter (quantified based on the write count) and writes blocks to the segments of different temperature levels. Each user write promotes the LBA to a hotter segment while each GC write demotes the LBA to a colder segment. Other temperature-based data placement schemes follow the similar idea of DAC, and mainly differ in the definition of per-LBA temperature-based counters and the promotion/demotion of LBAs across segments. Note that the above existing schemes are mainly designed for mitigating the flash-level WA in SSDs, yet they are also applicable for general log-structured storage.

We also consider three baseline strategies.

- **NoSep** appends any written blocks (either user-written blocks or GC-rewritten blocks) to the same open segment.
- **SepGC [31]** separates written blocks by user-written blocks and GC-rewritten blocks, and writes them into two different open

segments.

- **Future knowledge (FK)** assumes that the BIT of each written block is known in advance. For a written block (either a user-written block or a GC-rewritten block), if its invalidation will occur within t bytes since the written time, we write the block to the $\lceil \frac{t}{s} \rceil$ -th open segment, where s is the segment size (in bytes). Given the limited number of open segments, FK uses the last open segment to store all user-written blocks and GC-rewritten blocks if their BITs do not belong to the prior open segments. In our evaluation, we annotate the lifespan of each block in the traces in advance, so that we can compute the BIT of the block at the user write time.

By default, we configure six classes (each containing one open segment) for data placement for all schemes, except for NoSep, SepGC, and ETI. For NoSep, we configure one class for all user-written and GC-rewritten blocks; for SepGC, we configure two classes, one for user-written blocks and one for GC-rewritten blocks; for ETI, we configure two classes for user-written blocks and one class for GC-rewritten blocks. For MQ, SFR, and WARCIP, as they focus on separating user-written blocks only, we configure five classes for user-written blocks and the remaining class for GC-rewritten blocks. For DAC, SFS, ML, FADaC, and FK, since they do not distinguish user-written blocks and GC-rewritten blocks, we let them use all six classes for all blocks. We adopt the default settings as described in the original papers of the existing schemes.

4.2 Trace Overview

We use the *public* block-level I/O traces from Alibaba Cloud [19] for our trace-driven evaluation. The traces contain I/O requests (in multiples of 4 KiB blocks) from 1,000 virtual disks, referred to as *volumes*, over a one-month period in January 2020. While the traces are from a single cloud provider, they actually comprise a variety of workloads (e.g., virtual desktops, web services, key-value stores, and relational databases), and hence are representative for us to evaluate SepBIT and other data placement schemes under diverse workloads.

A previous study [33] shows that log-structured storage can be built atop the block storage stack at Alibaba Cloud for load balancing. Based on this motivation, our evaluation treats each volume in the traces as a standalone volume in the log-structured storage system (§2.1). Each volume performs data placement and GC independently. Our goal is to mitigate the overall WA across all volumes.

We pre-process the traces for our evaluation as follows. We only consider write requests as they are the only contributors of WA. Since some volumes in the traces have limited write requests to trigger sufficient GC operations, we remove such volumes to avoid biasing our analysis. Specifically, we focus on the volumes with sufficient write requests: each volume has a write working set size (WSS) (i.e., the number of unique LBAs being written multiplied by the block size) above 10 GiB and a total write traffic size (i.e., the number of written bytes) above $2\times$ its write WSS. To this end, we select 186 volumes, which account for a total of over 90% of write traffic of all 1,000 volumes. The 186 volumes contain 10.9 billion write requests, 410.2 TiB of written data (with 390.2 TiB of updates), 20.3 TiB of write WSS (with 17.2 TiB of update WSS). Each of the

186 volumes has a write WSS ranging from 10 GiB to 1 TiB and a write traffic size ranging from 43 GiB to 36.2 TiB. Since the WSS varies across volumes, we configure the maximum storage space of each volume as $\frac{WSS}{1-GPT}$, where GPT denotes the GP threshold to trigger GC.

4.3 Results

Summary of findings. We summarize our major evaluation findings as follows.

- SepBIT achieves the lowest WA among all data placement schemes (except FK) for different segment selection algorithms (Exp#1), different segment sizes (Exp#2), and different GP thresholds (Exp#3). It also reduces the 75th percentiles of per-volume WAs over all 186 volumes. In particular, when the segment size is small, SepBIT even has a lower WA than FK (Exp#2).
- We provide a breakdown analysis on SepBIT, and show its effectiveness of achieving a low WA by performing separation on each set of user-written blocks and GC-rewritten blocks independently (Exp#4).
- We provide a memory overhead analysis and show that SepBIT achieves low memory overhead for majority of volumes (Exp#5).

Default GC policy. Our default GC policy uses Cost-Benefit [24, 25] for segment selection and fixes the segment size and the GP threshold for triggering GC as 512 MiB and 15%, respectively. In Exps#1-#3, we vary each of the configurations to evaluate different data placement schemes.

Exp#1 (Impact of segment selection). We compare SepBIT with existing data placement schemes using Greedy [24] and Cost-Benefit [24, 25] for segment selection in GC (§2.1).

Figures 12(a) and 12(b) depict the overall WA across all 186 volumes under Greedy and Cost-Benefit, respectively. With separation in data placement, SepBIT reduces the overall WA of NoSep by 28.5% and 39.8% under Greedy and Cost-Benefit, respectively. More importantly, SepBIT achieves the lowest WA compared to all existing data placement schemes (except FK). It reduces the overall WA of SepGC and the eight state-of-the-art data placement schemes (i.e., excluding NoSep and FK) by 8.6-15.9% and 9.1-20.2% under Greedy and Cost-Benefit, respectively. Compared to FK, the overall WA of SepBIT is 13.5% and 3.1% higher under Greedy and Cost-Benefit, respectively. In short, SepBIT is highly efficient in WA mitigation under real-world workloads. Note that some data placement schemes even show a higher WA than SepGC, which performs simple separation of user-written blocks and GC-rewritten blocks, mainly because they fail to effectively group blocks with similar BITs (§2.3).

Figures 12(c) and 12(d) further show the boxplots of per-volume WAs over all 186 volumes under Greedy and Cost-Benefit, respectively (we omit some outliers of NoSep with very high WAs). SepBIT has the lowest 75th percentiles (1.61 and 1.36) among all existing data placement schemes (except FK) under Greedy and Cost-Benefit, while the second lowest one is DAC (1.64 and 1.50), respectively. This shows that the WA reduction of SepBIT is effective in individual volumes with diverse workloads. In particular, Cost-Benefit is more effective in the WA mitigation of SepBIT than Greedy, as the gap of the 75th percentiles between SepBIT and the second lowest one increases from 1.8% in Greedy to 9.4% in Cost-Benefit.

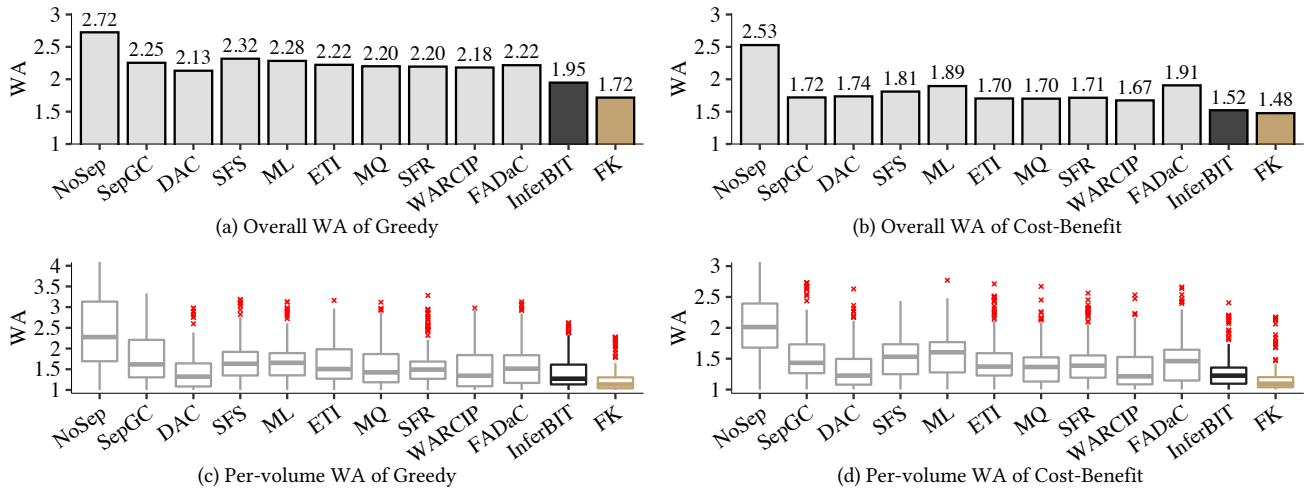


Figure 12: Exp#1 (Impact of segment selection).

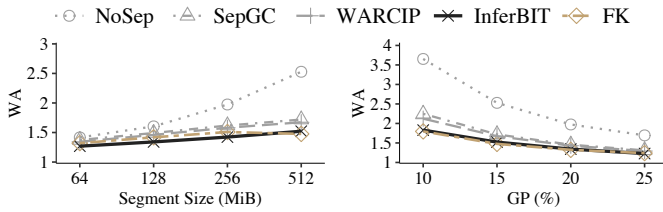


Figure 13: Exp#2 (Impact of segment sizes).

Figure 14: Exp#3 (Impact of GP thresholds).

Compared to FK, for 75th percentiles, SepBIT has 23.6% and 12.9% higher WA under Greedy and Cost-Benefit, respectively.

Exp#2 (Impact of segment sizes). We vary the segment size from 64 MiB to 512 MiB. For fair comparisons, we fix the amount of data (both valid and invalid data) to be retrieved in each GC operation as 512 MiB, meaning that a GC operation collects eight, four, two, and one segment(s) for the segment sizes of 64 MiB, 128 MiB, 256 MiB, and 512 MiB, respectively. We focus on comparing NoSep, SepGC, WARCIP, SepBIT, and FK, as they show the lowest WAs among existing data placement schemes for various segment sizes.

Figure 13 depicts the overall WA versus the segment size. Overall, using a smaller segment size yields a lower WA, as a GC operation can perform more fine-grained selection of segments for more efficient space reclamation. Again, SepBIT achieves the lowest WA compared to all existing data placement schemes; for example, its WA is with 5.5%, 8.2%, and 10.0% lower than WARCIP for the segment sizes of 64 MiB, 128 MiB, and 256 MiB, respectively. Interestingly, SepBIT even has a lower WA (by 3.9-5.7%) than FK when the segment size is in the range of 64 MiB to 256 MiB. The reason is that FK currently groups blocks of close BITs in five open segments, while the last open segment stores all blocks (we now configure six classes in total) (§4.1). If the segment size is smaller, FK can only group fewer blocks in the limited number of open segments, so it becomes less effective of grouping blocks of close BITs.

Exp#3 (Impact of GP thresholds). We vary the GP thresholds from 10% to 25%. We again focus on comparing the overall WAs

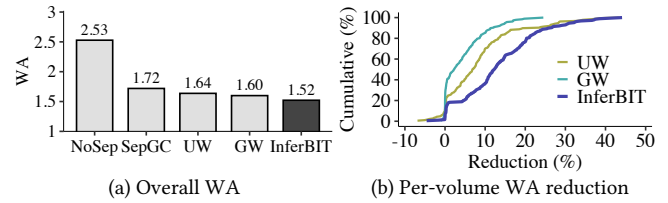


Figure 15: Exp#4 (Breakdown analysis).

of NoSep, SepGC, WARCIP, SepBIT, and FK as in Exp#2. Figure 14 shows the overall WA versus the GP threshold. A larger GP threshold has a lower WA in general, as it is easier for a GC operation to select segments with high GPs. SepBIT still shows the lowest WA. It has 5.0-13.8% lower WAs than WARCIP for different GP thresholds. Compared to FK, SepBIT has comparable WAs with differences smaller than 1.8%, for different GP thresholds.

Exp#4 (Breakdown analysis). We analyze how different components of SepBIT contribute to the WA mitigation. Recall that SepBIT separates written blocks into user-written blocks and GC-rewritten blocks, and further separates each set of user-written blocks and GC-rewritten blocks independently. In our breakdown analysis, we consider NoSep (i.e., without separation) and SepGC (i.e., which separates written blocks into user-written blocks and GC-rewritten blocks). We further consider two variants:

- **UW:** It further separates user-written blocks based on SepGC, but without separating GC-rewritten blocks. It maintains three classes: Classes 1 and 2 store short-lived blocks and long-lived blocks as in SepBIT, respectively, while Class 3 stores all GC-rewritten blocks.
- **GW:** It further separates GC-rewritten blocks based on SepGC, but without separating user-written blocks. It maintains four classes: Class 1 stores all user-written blocks, and Classes 2-4 store GC-rewritten blocks as in Classes 4-6 of SepBIT.

Figure 15(a) shows the overall WAs of different data placement schemes. Compared to NoSep, UW and GW reduce WA by 35.2% and 36.7%, respectively; compared to SepGC, UW and GW reduce

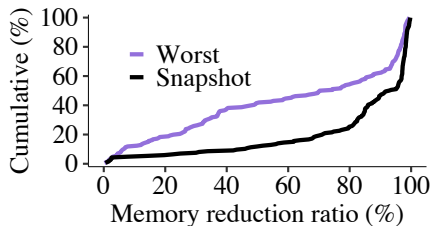


Figure 16: Exp#5 (Memory overhead analysis).

WA by 4.8% and 7.0%, respectively. The findings show that more fine-grained separation of each set of user-written blocks and GC-rewritten blocks brings further WA reduction. SepBIT achieves 7.0% and 4.9% WA reduction compared to UW and GW, respectively, thereby showing that SepBIT successfully combines the advantages brought by UW and GW.

Figure 15(b) further shows the cumulative distributions of the WA reductions of UW, GW, and SepBIT compared to SepGC across all volumes. We see that UW, GW, and SepBIT can reduce the WA of most of the volumes. The 75th percentiles of reductions of UW and GW are 11.4% and 6.9%, respectively, and their highest WA reductions are 43.3% and 24.5%, respectively. By combining UW and GW together, the 75th percentiles of the WA reductions of SepBIT compared to SepGC improves to 19.3% with highest WA reduction as 44.1%.

Exp#5 (Memory overhead analysis). We analyze the memory overhead of SepBIT in real-world workloads. Recall that SepBIT only needs to track the unique LBAs inside the FIFO queue (§3.4), instead of maintaining mappings for all LBAs in the write working set. We report the memory overhead reduction of SepBIT as one minus the ratio of the number of unique LBAs in the FIFO queue to the number of unique LBAs in the write working set. To quantify the reduction, for each volume, we collect all values of the number of unique LBAs in the FIFO queue in runtime when ℓ (defined in §3.4) is updated. To avoid bias due to the cold start of simulation, for each volume, we exclude the beginning 10% of the values. We also collect the number of unique LBAs at the end of simulation. We consider two cases, namely (i) the worst case and (ii) the snapshot case. In the worst case, we use the maximum number of unique LBAs in the FIFO queue for all volumes; it assumes that each volume has its peak number of unique LBAs in the FIFO queue and incurs the most memory. In the snapshot case, we use the number of unique LBAs at the end of the simulation; it represents a snapshot of the system status.

From our analysis, we find that in the worst case, SepBIT reduces the overall memory overhead by 44.8%, while in the snapshot case, SepBIT reduces the overall memory overhead by 71.8%. To calculate the actual memory overhead, suppose that the mapping for each LBA costs 8 bytes. Since the aggregated write WSS of the 186 volumes is 20.3 TiB (§4.2), SepBIT reduces the overall memory overhead from $20.3 \cdot \frac{2^{40}}{2^{12}} \cdot 8 = 41.6$ GiB to $41.6 \cdot (1 - 71.8\%) = 11.7$ GiB.

Figure 16 further depicts the cumulative distribution of the memory overhead reductions across volumes under both the worst case and the snapshot case. In the worst case, SepBIT reduces the memory overhead by more than 72.3% in half of the volumes and the highest memory overhead reduction is 99.5%; in the snapshot case,

the median reduction is 93.1% with the highest reduction as 99.7%. The reason of the differences among volumes is due to their different degrees of skewness. The volumes with higher skewness see more aggregated traffic patterns, and hence the number of recently updated LBAs is much smaller compared to their write WSS.

5 RELATED WORK

In this section, we review related work on GC designs for different log-structured storage systems.

GC in SSDs. We evaluated several existing data placement schemes (§4.1) for mitigating the WA of flash-level GC in SSDs. Other data placement schemes build on the use of program contexts [15] or the prediction of block temperature based on neural networks [38]. Some empirical studies evaluate the data placement algorithms on an SSD platform [18], or characterize how real-world I/O workloads affect GC performance [34]. In particular, Yadgar et al. [34] also investigate the impact of the number of separated classes in data placement based on the temperature-based data scheme in [29]. In contrast, SepBIT builds on the BIT for data placement, backed by the empirical studies from real-world I/O traces.

Besides data placement, existing studies propose segment selection algorithms to reduce the WA of flash-level GC. In addition to Greedy and Cost-Benefit (§2.1), Cost-Age-Times [6] considers the cleaning cost, data age, and flash erasure counts in segment selection. Windowed Greedy [13], Random-Greedy [20], and d-choices [30] are variants of Greedy in segment selection. Desnoyers [9] models the WA of different segment selection algorithms and hot-cold data separation. SepBIT can be used in conjunction with existing segment selection algorithms.

GC in file systems. Several studies examine the GC performance for log-structured file systems. Matthew et al. [21] improve the GC performance by adapting GC to the system and workload behaviors. SFS [22] separates blocks by hotness (i.e., write frequency divided by age). Some reduce WA using file system hints in data placement; for example, WOLF [32] groups blocks by files or directories, while hFS [39] and F2FS [17] separate data and metadata. Besides WA reduction, some studies focus on mitigating the GC interference [3] and fragmentation in log-structured file systems [10, 23, 37].

GC for RAID and distributed storage. Some studies address the GC performance issues in RAID and distributed storage, such as reducing the WA of Log-RAID systems [8] and mitigating the interference between GC and user writes via GC scheduling in RAID arrays [15, 28]. RAMCloud [25] targets persistent distributed in-memory storage. It proposes two-level cleaning to maximize memory utilization by coordinating the GC operations in memory and disk backends. It also corrects the original Cost-Benefit algorithm [24] for accurate segment selection.

6 CONCLUSION

We propose SepBIT, a novel data placement scheme that mitigates WA caused by GC in log-structured storage by grouping blocks with similar estimated BITs. Inspired from the ideal data placement that minimizes WA (i.e., WA=1) using future knowledge of BITs, SepBIT leverages the skewed write patterns of real-world workloads to infer BITs. It separates written blocks into user-written blocks and GC-rewritten blocks and performs fine-grained separation in each

set of user-written blocks and GC-rewritten blocks. To group blocks with similar BITs, it infers the BITs of user-written blocks and GC-rewritten blocks by estimating their lifespans and residual lifespans, respectively. Evaluation on the block-level I/O traces from Alibaba Cloud shows that SepBIT achieves the lowest WA compared to eight state-of-the-art data placement schemes.

REFERENCES

- [1] N. Agrawal, V. Prabhakaran, T. Wobber, J. D. Davis, M. S. Manasse, and R. Panigrahy. Design tradeoffs for SSD performance. In *Proc. of USENIX FAST*, 2008.
- [2] M. Balakrishnan, D. Malkhi, J. D. Davis, V. Prabhakaran, M. Wei, and T. Wobber. CORFU: A distributed shared log. *ACM Trans. on Computer Systems*, 31(4):10, 2013.
- [3] T. Blackwell, J. Harris, and M. I. Seltzer. Heuristic cleaning algorithms in log-structured file systems. In *Proc. of USENIX ATC*, 1995.
- [4] F. Chang, J. Dean, S. Ghemawat, W. C. Hsieh, D. A. Wallach, M. Burrows, T. Chandrasekaran, A. Fikes, and R. E. Gruber. Bigtable: A distributed storage system for structured data. In *Proc. of USENIX OSDI*, 2006.
- [5] F. Chen, D. A. Koufaty, and X. Zhang. Understanding intrinsic characteristics and system implications of flash memory based solid state drives. In *Proc. of ACM SIGMETRICS*, Jun 2009.
- [6] M. Chiang and R. Chang. Cleaning policies in mobile computers using flash memory. *Journal of Systems and Software*, 48(3):213–231, 1999.
- [7] M.-L. Chiang, P. C. Lee, and R.-C. Chang. Using data clustering to improve cleaning performance for flash memory. *Software: Practice and Experience*, 29(3):267–290, 1999.
- [8] T.-c. Chiueh, W. Tsao, H.-C. Sun, T.-F. Chien, A.-N. Chang, and C.-D. Chen. Software orchestrated flash array. In *Proc of ACM SYSTOR*, 2014.
- [9] P. Desnoyers. Analytic models of SSD write performance. *ACM Trans. on Storage*, 10(2):1–25, 2014.
- [10] S. S. Hahn, S. Lee, C. Ji, L.-P. Chang, I. Yee, L. Shi, C. J. Xue, and J. Kim. Improving file system performance of mobile storage systems using a decoupled defragmenter. In *Proc. of USENIX ATC*, 2017.
- [11] J. H. Hartman and J. K. Ousterhout. The zebra striped network file system. In *Proc. of ACM SOSP*, 1993.
- [12] J. He, S. Kannan, A. C. Arpaci-Dusseau, and R. H. Arpaci-Dusseau. The unwritten contract of solid state drives. In *Proc. of ACM EuroSys*, 2017.
- [13] X. Hu, E. Eleftheriou, R. Haas, I. Iliadis, and R. Pletka. Write Amplification Analysis in Flash-based Solid State Drives. In *Proc. of ACM SYSTOR*, 2009.
- [14] J. Kim, K. Lim, Y. Jung, S. Lee, C. Min, and S. H. Noh. Alleviating garbage collection interference through spatial separation in all flash arrays. In *Proc. of USENIX ATC*, 2019.
- [15] T. Kim, D. Hong, S. S. Hahn, M. Chun, S. Lee, J. Hwang, J. Lee, and J. Kim. Fully automatic stream management for multi-streamed SSDs using program contexts. In *Proc. of USENIX FAST*, 2019.
- [16] K. Kremer and A. Brinkmann. FADaC: a self-adapting data classifier for flash memory. In *Proc. of ACM SYSTOR*, 2019.
- [17] C. Lee, D. Sim, J. Hwang, and S. Cho. F2FS: A new file system for flash storage. In *Proc. of USENIX FAST*, 2015.
- [18] J. Lee and J.-S. Kim. An empirical study of hot/cold data separation policies in solid state drives (SSDs). In *Proc. of ACM SYSTOR*, 2013.
- [19] J. Li, Q. Wang, P. P. C. Lee, and C. Shi. An in-depth analysis of cloud block storage workloads in large-scale production. In *Proc. of IEEE IISWC*, 2020.
- [20] Y. Li, P. P. C. Lee, and J. C. S. Lui. Stochastic modeling of large-scale solid-state storage systems: Analysis, design tradeoffs and optimization. In *Proc. of ACM SIGMETRICS*, 2013.
- [21] J. N. Matthews, D. S. Roselli, A. M. Costello, R. Y. Wang, and T. E. Anderson. Improving the performance of log-structured file systems with adaptive methods. In *Proc. of ACM SOSP*, 1997.
- [22] C. Min, K. Kim, H. Cho, S.-W. Lee, and Y. I. Eom. SFS: random write considered harmful in solid state drives. In *Proc. of USENIX FAST*, 2012.
- [23] J. Park, D. H. Kang, and Y. I. Eom. File defragmentation scheme for a log-structured file system. In *Proc. of ACM APSys*, 2016.
- [24] M. Rosenblum and J. K. Ousterhout. The design and implementation of a log-structured file system. *ACM Trans. on Computer Systems*, 10(1):26–52, 1992.
- [25] S. M. Rumble, A. Kejriwal, and J. Ousterhout. Log-structured memory for DRAM-based storage. In *Proc. of USENIX FAST*, 2014.
- [26] M. I. Seltzer, K. Bostic, M. K. McKusick, and C. Staelin. An implementation of a log-structured file system for UNIX. In *Proc. of USENIX ATC*, 1993.
- [27] M. Shafaei, P. Desnoyers, and J. Fitzpatrick. Write amplification reduction in flash-based SSDs through extent-based temperature identification. In *Proc. of USENIX HotStorage*, 2016.
- [28] J. Y. Shin, M. Balakrishnan, T. Marian, and H. Weatherspoon. Gecko: Contention-oblivious disk arrays for cloud storage. In *Proc. of USENIX FAST*, 2013.
- [29] R. Stoica and A. Ailamaki. Improving flash write performance by using update frequency. *Proc. of the VLDB Endowment*, 6(9):733–744, 2013.
- [30] B. Van Houdt. A mean field model for a class of garbage collection algorithms in flash-based solid state drives. *ACM SIGMETRICS Performance Evaluation Review*, 41(1):191–202, 2013.
- [31] B. Van Houdt. On the necessity of hot and cold data identification to reduce the write amplification in flash-based SSDs. *Performance Evaluation*, 82:1–14, 2014.
- [32] J. Wang and Y. Hu. WOLF - A novel reordering write buffer to boost the performance of log-structured file systems. In *Proc. of USENIX FAST*, 2002.
- [33] E. Xu, M. Zheng, F. Qin, Y. Xu, and J. Wu. Lessons and actions: What we learned from 10k SSD-related storage system failures. In *Proc. of USENIX ATC*, 2019.
- [34] G. Yadgar, M. Gabel, S. Jaffer, and B. Schroeder. SSD-based workload characteristics and their performance implications. In *ACM Trans. on Storage*, 2021.
- [35] J. Yang, R. Pandurangan, C. Choi, and V. Balakrishnan. AutoStream: automatic stream management for multi-streamed SSDs. In *Proc. of ACM SYSTOR*, 2017.
- [36] J. Yang, S. Pei, and Q. Yang. WARCIP: write amplification reduction by clustering I/O pages. In *Proc. of ACM SYSTOR*, 2019.
- [37] L. Yang, F. Wang, Z. Tan, D. Feng, J. Qian, and S. Tu. ARS: Reducing F2FS fragmentation for smartphones using decision trees. In *Proc. of ACM DATE*, 2020.
- [38] P. Yang, N. Xue, Y. Zhang, Y. Zhou, L. Sun, W. Chen, Z. Chen, W. Xia, J. Li, and K. Kwon. Reducing garbage collection overhead in SSD based on workload prediction. In *Proc. of USENIX HotStorage*, 2019.
- [39] Z. Zhang and K. Ghose. hFS: A hybrid file system prototype for improving small file and metadata performance. In *Proc. of EuroSys*, 2007.